Has the risk of a 1976 north-west European summer drought and heatwave event increased since the 1970s due to climate change?

Received: 17 December 2020 | Revised: 19 July 2021 | Accepted: 21 September 2021

DOI: 10.1002/qj.4172

Quarterly Journal of the Royal Meteorological Society RMetS

RESEARCH ARTICLE

Has the risk of a 1976 north-west European summer drought and heatwave event increased since the 1970s because of climate change?

Laura Baker | **Len Shaffrey** | **Ed Hawkins**

National Centre for Atmospheric Science, Department of Meteorology, University of Reading, Reading, UK

Correspondence
L. Baker, National Centre for Atmospheric Science, Department of Meteorology, University of Reading, Reading, RG6 6BB, UK
Email: l.h.baker@reading.ac.uk

Funding information
NERC EUPHEME National Centre for Atmospheric Science, Grant/Award Numbers: NE/L010488/1, 690462

Abstract

In the summer of 1976, north-west Europe experienced an exceptional heatwave and drought, which impacted agriculture and public water supply. This study aims to assess how the likelihood of the event in the present-day climate has changed since 1976 because of climate change. The analysis focuses on the England and Wales region, which was particularly badly impacted. Three key factors contributing to the extreme summer were identified: the dry preceding winter–spring period, the dry summer and the hot summer. Following the principles of event attribution, three methods are used to evaluate the change in event risk: one using observational data, a second using CMIP5 coupled climate models and a third using HadGEM3-A atmosphere-only simulations. This is the first time that this method has been used to evaluate how the risk of a historical extreme event has changed since it originally occurred. The results from the three methods agree qualitatively. The probability of a summer at least as hot as 1976 has increased significantly between the 1970s and the present-day climate (estimated risk ratios 11 (5–95% confidence interval (CI) [7,14]), 9 (CI [4,28]) and 19 (CI [5,25]) based on the three respective methods). In contrast, no significant change in the probability of an extreme dry winter–spring or an extreme dry summer was found. However, the joint probability of an extreme dry winter–spring followed by an extreme hot summer and the probability of an extreme hot and dry summer have both increased significantly between the 1970s and the present day (estimated risk ratios between 5 and 79, and between 3 and 39, respectively). Water resource systems should therefore be robust enough to cope with more frequent occurrences of summers as extreme as 1976.

KEYWORDS

attribution, climate change, drought, extreme, heatwave, risk

1 | INTRODUCTION

Summer heatwaves and prolonged periods of low rainfall leading to drought have serious implications for many sectors, including water resource management, agriculture and human health. One of the most notable such events in the UK and north-west Europe, and the topic of this study, is the 1975/1976 drought and heatwave. The summer of 1976 is well remembered within the UK for being exceptionally hot, with much of the country experiencing severe drought due to exceptionally low rainfall in the summer and the preceding months. The period May 1975 to August 1976 had the lowest 16-month rainfall in the England and Wales series on record (Marsh *et al.*, 2007), with some areas of England receiving less than 50% of the average (over the period 1916–1950) rainfall (Rodda and Marsh, 2011). The exceptionally dry winter of 1975/1976 meant that reservoirs, lakes and aquifers, which form the basis of the UK's water supply system, did not recharge as they normally do over the winter period. This led to reductions in available water for agriculture, industry and public water supply (Murray, 1977). In the UK, the event is widely considered by water boards and contingency planners as a benchmark drought event (Marsh *et al.*, 2007; Rodda and Marsh, 2011), since it resulted in surface water and ground water reserves becoming significantly depleted. In the UK, the biggest impacts were in England and Wales. Western continental Europe was also exceptionally hot and dry (Stubbs, 1977). The reduction in water availability resulted in severe restrictions on water usage. This had significant impacts on the agricultural sector, which saw a large reduction in productivity; industry, which was forced to reuse water; and the public, with widespread hosepipe bans, standpipes and in some places the public water supply being turned off entirely for parts of the day or night (Rodda and Marsh, 2011; Taylor *et al.*, 2009).

The prolonged period of low rainfall and the hot summer of 1976 were associated with the North Atlantic jet being shifted to the north (Ratcliffe, 1977). This was accompanied by anticyclonic conditions and blocking over the UK and north-west Europe, bringing warm and dry conditions to this region. The sea-surface temperatures (SSTs) in the sub-polar gyre were colder than average, with warm SST anomalies in the mid-North Atlantic (Dunstone *et al.*, 2019).

There have been several other hot summers since 1976, but even in the context of the warming climate, 1976 still stands out as an extreme event. Recent hot summers in the UK include 2003, 2006 and 2018. Dunstone *et al.* (2019) showed similarities between the atmospheric circulation patterns and North Atlantic sea-surface temperatures in the summers of 2018 and 1976. The summer mean temperatures for England and for the UK as a whole were actually slightly warmer in 2018 than 1976 (Kendon *et al.*, 2019). However, it was the combination of the exceptionally hot, dry summer and the preceding very dry period that resulted in the severe impacts of the event.

Given that the 1976 event occurred within living memory for many people, there is potentially an inherent assumption that the likelihood of such an event may not have changed since then. However, an important question is whether the probability and characteristics of such an extreme event have changed since the 1970s because of anthropogenic climate change. If they have, then this has implications for water resource management and drought planning. This is the first published study to look at how the likelihood of a historical extreme event that is still used as a benchmark for planning purposes may have changed since its occurrence several decades ago.

Kendon *et al.* (2020) summarised the recent changes in UK climate based on observational analysis and showed that, overall, the UK has in general become warmer and wetter. They found the UK-average annual-mean temperature in the decade 2010–2019 was 0.9 K warmer than the average for the period 1961–1990, and had increased in all four seasons. Notably for the present study, the UK summer mean temperature has increased by 0.8 K between these two periods. The Central England Temperature series shows a 0.7 K increase in annual temperature. Annual rainfall in the whole UK has increased by 5% between 1961–1990 and 2010–2019, with the largest increase seen in Scotland. Seasonally, the winters and summers have become wetter (12% and 13%, respectively), while spring and autumn have become slightly drier. In the England and Wales region, 2010–2019 was 7% wetter than in 1961–1990.

Given the recent observed changes in UK climate, we aim to assess the change in the probability of a 1975/1976-type drought and heatwave event occurring in the current (2011–2020) climate compared with the 1970s (1971–1980) climate. The methodology used here applies the principles of event attribution to give observational and model-based estimates of these changes.

Event attribution is a rapidly growing area of research. There have been many studies aiming to assess the impact that anthropogenic climate change has had on the probability of specific events, such as heatwaves (e.g., Stott *et al.*, 2004; Lewis and Karoly, 2013; Sippel *et al.*, 2016; Wilcox *et al.*, 2018), drought (e.g., Williams *et al.*, 2015; Hauser *et al.*, 2017) and extreme precipitation events (e.g., Pall *et al.*, 2011; Schaller *et al.*, 2016; Otto *et al.*, 2018; Wilcox *et al.*, 2018). In attribution studies, the probability of a given event occurring in the present-day climate is compared with the probability of the event occurring in a natural or counterfactual climate, in which anthropogenic climate change has not occurred. This change

in probability is typically estimated using climate model simulations. The event probability is estimated from climate model simulations of the present-day climate and compared with the event probability in an equivalent set of simulations in a natural or counterfactual climate, in which greenhouse gases are set to pre-industrial levels, (e.g., Stott *et al.*, 2016). Another method of event attribution is to use observations to assess the change in probability of the event in the present compared with an earlier period (e.g., Wilcox *et al.*, 2018).

In the present study, we use the techniques of attribution studies, but instead of comparing present-day and counterfactual climates (i.e., with and without anthropogenic emissions), we assess the change in probability of the 1975/1976 heatwave and drought event between the climate of 1976 and the present-day climate. Three different approaches are used to do this: one using observations, a second using coupled climate model simulations (CMIP5) and a third using atmosphere-only simulations (HadGEM3-A) with prescribed sea-surface temperatures (SSTs).

The objectives of this study are:

- To define the 1975/1976 drought event in terms of its three key components, namely the dry winter–spring period, the dry summer and the hot summer of 1976;
- To evaluate the probability of the event occurring in the climate of 1975/1976 using observations and climate model experiments;
- To evaluate the change in probability of the event in the present-day climate compared with the 1975/1976 climate.

In Section 2, the different methodologies used to calculate the event probability, using observations and climate models, are described. In Section 3, the observed 1975/1976 drought event is described and defined. In Section 4, the results from the observation-based and climate model-based evaluation of event probabilities are presented. An evaluation of joint probabilities of different components of the event is given in Section 5. Finally, the conclusions and a discussion of the implications of these results are given in Section 6.

2 | METHODOLOGY

2.1 | Calculating extreme event probabilities using observations

The observational estimate of the event probability is derived using the methodology of Hawkins *et al.* (2020), in which local variations in climate are linearly regressed onto annual global mean surface temperature change to give a signal and a noise component. The local change in climate is given by

$$L(t) = \alpha G(t) + \beta \tag{1}$$

where $L(t)$ is the local change over time, $G(t)$ is the smoothed global mean surface temperature change over the same period, α is a linear scaling and β is a constant. In this study, the local change $L(t)$ represents the summer (JJA) mean temperature, the JJA mean precipitation or the winter–spring (DJFMAM) mean precipitation in the England and Wales region. The smoothing of $G(t)$ is done with a lowess filter of 41 years to highlight the long-term variation. The local climate change signal at a given time is αG and the residuals are $(L - \alpha G)$. Using the regression in equation 1, we simulate a random variable with the parameters estimated from the residuals of the linear fit, similar to the method used by Vautard *et al.* (2020), van Oldenborgh *et al.* (2019), van Oldenborgh *et al.* (2021), for example. For JJA temperature, a generalised extreme value (GEV) distribution is fitted to the residuals. This was chosen because it had a better fit to the residuals than a Gaussian distribution, and we note that there is some sensitivity of the results to the choice of fitted distribution owing to the limited sample size of the observations. For JJA and DJFMAM precipitation, a normal distribution with mean $L(t)$ and standard deviation $(L - \alpha G)$ is used. This distribution is commonly used for seasonal precipitation, for example, Wilcox *et al.* (2018). These derived distributions of observations are then used to calculate the probability of an event (e.g., an exceedance of a threshold) at a specified time. In the present study, the event probabilities are evaluated for the years 1976 and 2019. The method described here was used for the analysis presented in Section 4.1.

The observational data used to derive these temperature and precipitation distributions are the mean temperature and rainfall for the England and Wales region from the Met Office HadUK 1 km observations, for the period 1862–2019 (for rainfall) and 1884–2019 (for temperature). For $G(t)$, the global mean surface temperature from the Berkeley Earth temperature dataset for 1850–2019 (Rohde *et al.*, 2013) combined with HadSST3 from Kennedy *et al.* (2011) are used.

2.2 | Calculating extreme event probabilities using climate models

2.2.1 | Coupled model simulations

To estimate the change in probability of the event using coupled models, data from the fifth Coupled Model

Intercomparison Project (CMIP5) (Taylor *et al.*, 2012) are used. Data from the historical simulations for the period 1971–1980 are used to represent the 1970s climate, and data from the RCP4.5 simulations for the period 2011–2020 are used to represent the present-day climate. A single ensemble member (the first member in models with more than one) from each of the 15 models listed in Table S1 was used to ensure that each model had equal weighting, resulting in 150 model years for each period. All CMIP5 model data are re-gridded to the same N96 grid used for the HadGEM3-A simulations (see below). Data for each model were bias-corrected by subtracting the difference between each model's mean value and the multi-model mean value for each 10-year period.

2.2.2 | HadGEM3-A simulations

To estimate the event probabilities using atmosphere-only model simulations, two sets of simulations were performed with the HadGEM3-A system (Walters *et al.*, 2011) at N96 L85 resolution (1.25° longitude by 1.875° latitude; model top at 85 km). The model was run with the GA7 atmosphere, which uses the ENDGame dynamical core and the Joint UK Land Environment Simulator (JULES) land surface model (Walters *et al.*, 2019). SSTs and sea-ice fields were prescribed for each month, as described below.

A set of 150 simulations of 12 months (from November to October) was performed to represent the 1976 event. In this case, the SSTs and sea ice were prescribed for each month from November 1975 to October 1976, using HadISST observed monthly values (Rayner *et al.*, 2003). The greenhouse gas concentrations for 1976 were taken from the IPCC AR5 Annex II (Stocker *et al.*, 2014). CMIP6 aerosol emissions for 1976 were used, except for biomass burning emissions, which used a fixed monthly climatology for the period 2002–2011 from the Global Fire Emissions Database (GFED). Ozone was prescribed as a 2D climatology for the period 1994–2005 for each month. Individual ensemble members differ by differences in their initial conditions; the chaotic nature of the modelled atmosphere means that the members quickly diverge despite having the same lower boundary forcing from the prescribed SSTs and sea ice. The results from the HadGEM3-A experiments are therefore conditional on 1976 SST anomalies, which is addressing a slightly different question to the analysis of the CMIP5 data which are not conditional on particular SSTs.

A second set of 150 simulations of 12 months was performed to represent the 1976 event in the current climate. To do this, the SSTs, aerosol emissions and greenhouse gas concentrations were perturbed to reflect the current climate. The SST perturbation was made by subtracting the 1971–1980 mean SSTs for each month from the 2011–2020 means. These values were taken as the multi-model mean of CMIP5 model estimates from the historical simulations and RCP4.5 scenario, respectively. Only the first ensemble member of each coupled model was used, in order to maximise the number of models and to give an equal weighting to each model, resulting in a mean over 15 models (Table S1). The importance of carefully choosing the SSTs has been highlighted for attribution studies (e.g., Wilcox *et al.*, 2018). However, in our experiments, since we only require SSTs for the present and recent past, the SSTs are better constrained than in attribution studies. For simplicity, sea ice was left at 1976 values. Since present-day sea ice is, in general, less extensive than in 1976, this means that these simulations may be missing a small amount of additional warming. We note that leaving the sea ice fixed in this way could impact the mean circulation. However, previous authors have found that the impact of sea ice was small for climate attribution studies (Schaller *et al.*, 2016), so these differences are likely to have only a small impact on the results. Greenhouse gas concentrations and aerosol emissions were set to 2010 levels (with the exception of biomass burning emissions and ozone, which were the same climatologies as above).

2.3 | Metrics used to evaluate the event probabilities and risk ratios

Before discussing the results, we first define the measures used to evaluate the event probabilities and risk ratios.

If we define an event E as the occurrence of a quantity exceeding a given threshold, then the probability of the event occurring in a set of N years is

$$p(E) = n_E/N$$

where n_E is the number of occurrences of event E.

The risk ratio RR gives a measure of the change in risk of the event between two datasets. In our case, we wish to evaluate the change in the event risk between the 1970s climate and the present-day climate. The risk ratio for event E is given by

$$RR(E) = p_{\text{present}}(E)/p_{1970\text{s}}(E).$$

The uncertainties in these quantities are given by the 5–95% confidence intervals, which are estimated using 1,000 standard bootstrap samples with replacement.

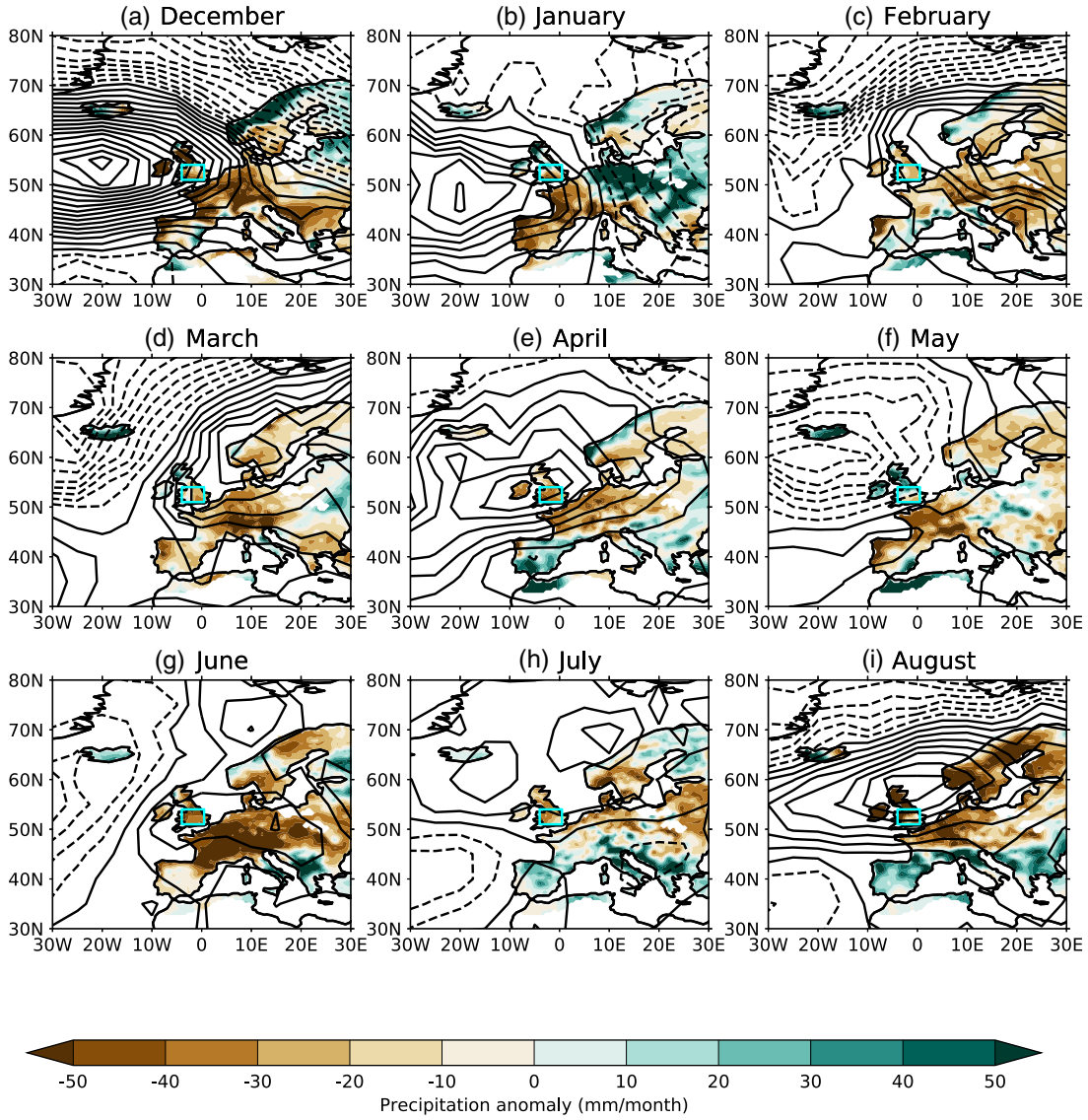

FIGURE 1 Anomalies of E-OBS precipitation (filled contours) and HadSLP2 MSLP (black contours every 1 hPa, negative values dashed), in each month from December 1975 to August 1976. Anomalies are with respect to the relevant month in the period 1950/1951 to 1999/2000 [Colour figure can be viewed at wileyonlinelibrary.com]

3 | AN OVERVIEW OF THE 1975/1976 DROUGHT AND HEATWAVE EVENT

In this section, the observed 1975/1976 drought and summer heatwave event is discussed. We focus on the period December 1975 to August 1976, in order to cover both the preceding winter–spring period, which is the most important in terms of water resource recharge, and the summer period, in which the dry conditions continued and the extreme hot temperatures occurred, resulting in the most severe impacts of the event.

The temperature and precipitation data used for the observational analysis in this section are derived from E-OBS observations of daily surface temperature and precipitation on a 0.5° regular grid (Haylock *et al.*, 2008). Monthly mean sea-level pressure data are from HadSLP2 (Allan and Ansell, 2006), on a 5° regular grid.

3.1 | Synoptic conditions

Over the period December 1975 to August 1976, the atmospheric flow over the UK and continental Europe was predominantly anticyclonic (Figure 1, black contours). This is consistent with the northward-shifted jet discussed previously. This resulted in drier-than-average conditions over the UK and north-west continental Europe in nearly all months (Figure 1), with precipitation anomalies of over 50 mm·month^{-1} less than average in some areas, most

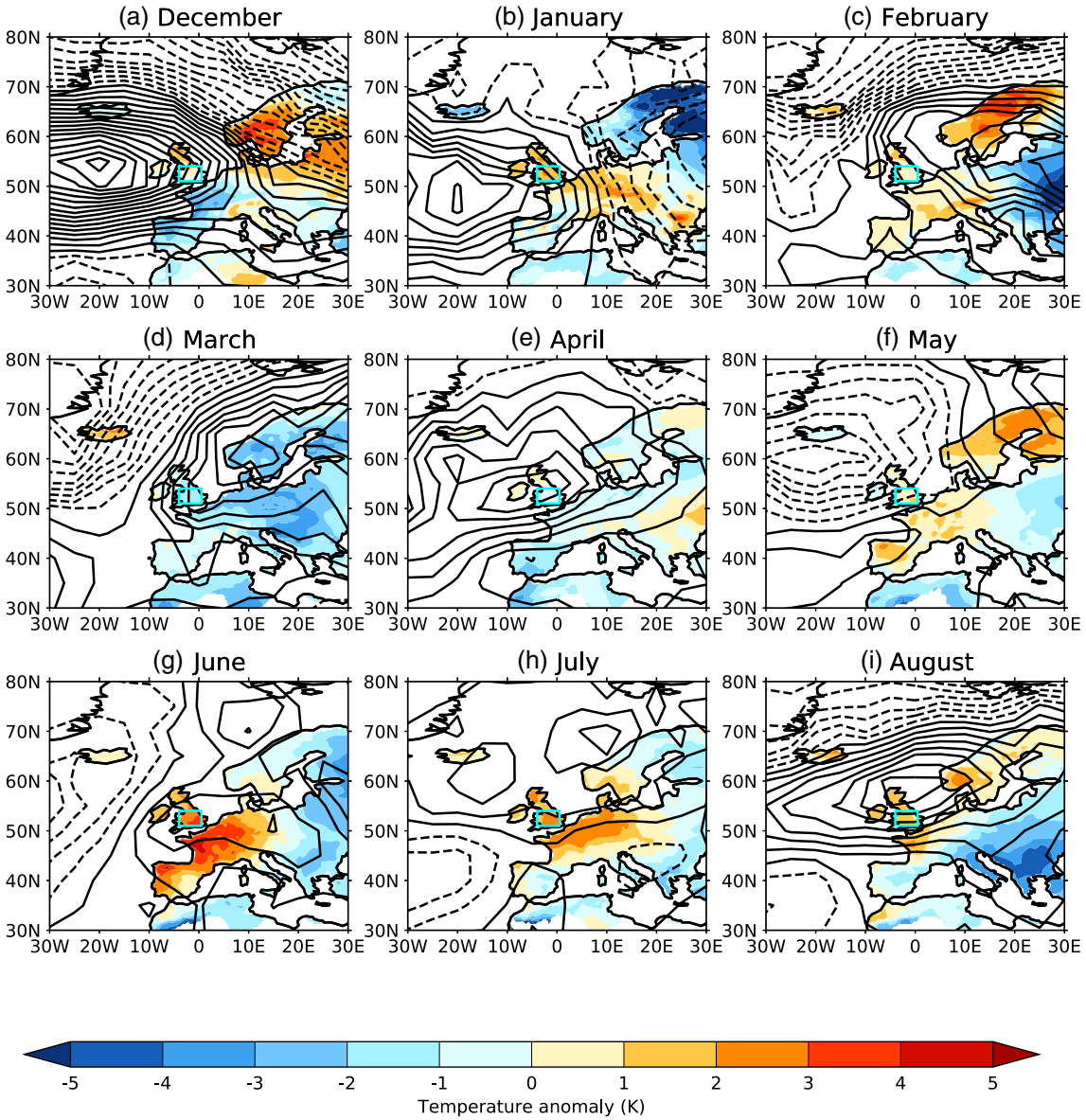

FIGURE 2 Observed anomalies of E-OBS surface temperature (filled contours) and HadSLP2 MSLP (black contours every 1 hPa, negative values dashed), in each month from December 1975 to August 1976. Anomalies are with respect to the relevant month in the period 1950/1951 to 1999/2000 [Colour figure can be viewed at wileyonlinelibrary.com]

notably in December, June and August. In contrast, southern Europe had wetter-than-average conditions for much of the late spring and summer. In winter, temperatures in the UK were warmer than average (Figure 2), while temperature anomalies elsewhere in Europe varied throughout the season as the position of the anticyclone shifted from west to east. Temperatures over most of Europe were colder than average in early spring, but from May onwards the temperatures in the UK and western continental Europe were consistently higher than average. Southern Europe was also warmer than average in May and June but then cooler for the remainder of the summer. The north–south division in precipitation and surface temperature anomalies in summer is consistent with the positive phase of the summer North Atlantic Oscillation (see Folland *et al.* (2009)).

3.2 | Time-series analysis for the England and Wales region

We now focus our analysis on the England and Wales region, which was the area of the UK most severely affected by the drought in summer 1976. For the model-based analysis in Section 4.2, a region covering England and Wales (51–54°N, 4°W–0.5°E; indicated in Figure 1; hereafter the EW region) was selected. The region is relatively small in order to exclude grid points in

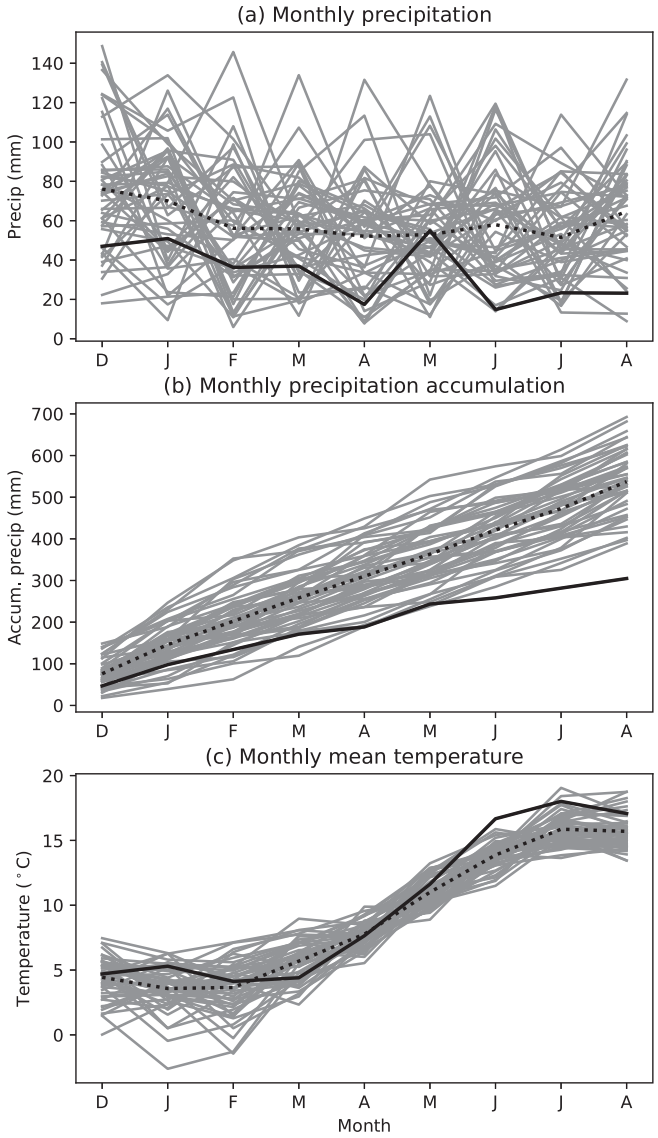

FIGURE 3 (a) Observed E-OBS precipitation, (b) precipitation accumulation from the start of December and (c) mean temperature in each month, for the EW region. Bold black lines show December 1975 to August 1976; bold black dotted lines show the mean for each month over all years between 1950/1951 and 1999/2000; and grey lines show all individual years in this period

the HadGEM3-A simulations containing any areas of sea, which will have lower variability than land points due to prescribing the SSTs.

Figure 3a shows observed time series of the total monthly precipitation averaged over the EW region, for the period December to August for all years in the period 1950/1951–1999/2000, with 1975/1976 highlighted in bold. It can be seen that the precipitation in 1975/1976 in all months was substantially lower than the mean, and was among the lowest few years in almost all months. Figure 3b shows the accumulated precipitation over this period. The total accumulation by May was just over half the mean for this period, and was the lowest winter–spring precipitation accumulation of all the years shown. As 1975 was also a relatively dry year (Perry, 1976), the groundwater levels and river flows were already low at the start of winter 1975. This left water levels exceptionally low by the end of spring 1976, impacting river, reservoir and groundwater levels. The summer months were also exceptionally dry: June 1976 was the driest June in the period shown (Figure 3a) and the precipitation in July and August was also very low, resulting in a 9-month rainfall accumulation by the end of August of around half the mean value (Figure 3b)—by far the lowest December–August 9-month accumulation in the 50-year observational record.

In the EW region, the temperatures in winter and spring 1975/1976 were generally around average (Figure 3c). However, the summer season was exceptionally hot. The June 1976 mean surface temperature was considerably hotter than in any other year shown (3.3 K warmer than the mean), July 1976 was the third-hottest year in the period and August 1976 was the seventh-hottest year.

3.3 | Defining the 1975/1976 drought event

To evaluate the probability of the 1975/1976 drought occurring, it is first necessary to determine a set of criteria that define the event. We consider the three key factors that contributed to the drought and water shortages in the England and Wales region in the summer of 1976. These are the winter–spring (DJFMAM) precipitation, the summer (JJA) mean precipitation and the summer mean temperature. To define the 1975/1976 event, we define thresholds of these three quantities in the EW region (mean over the box 51°–54°N, 4°W–0.5°E). We use the observed 1975/1976 anomalies of these quantities, relative to the mean of the observations for 1950/1951 to 1999/2000: dry winter–spring is defined as the DJFMAM mean precipitation anomaly less than $-20.1\ \text{mm}\cdot\text{month}^{-1}$; dry summer is defined as JJA mean precipitation anomaly less than $-37.5\ \text{mm}\cdot\text{month}^{-1}$; and hot summer is defined as the JJA mean temperature anomaly greater than 2.0 K.

An important question is whether these three components of the 1975/1976 drought can be considered independent. There are obvious links between concurrent temperature and precipitation variability in summer, both of which are driven largely by variations in the North Atlantic jet. Both hot summers and dry summers are typically linked to anticyclonic conditions. However, the relationship between winter–spring precipitation and summer temperature and precipitation are less clear. Dry

winter–spring periods can result in low soil moisture going into the summer season. Several studies have shown that low soil moisture can enhance extreme temperatures during heatwaves in central and south-eastern Europe (e.g., Vautard *et al.*, 2007; Stefanon *et al.*, 2012; Whan *et al.*, 2015). However, this will only occur when the soils are very dry, so in generally wetter regions, such as the UK, this enhancement will only occur in extreme drought conditions (Alexander, 2011), and so in these regions the relationship is less clear.

Given these uncertainties, we now examine the observed relationships between DJFMAM precipitation, JJA temperature and JJA precipitation for the EW region. There is no significant correlation between DJFMAM precipitation and JJA temperature (black lines in Figure 4a, correlation 0.05, $p > .7$). However, 1976 (marked by a black star) has the highest JJA temperature and one of the lowest DJFMAM precipitation values. In this case, it may be that the low soil moisture at the start of summer further increased the summer temperatures, which was also concluded by Fischer *et al.* (2007) based on their model sensitivity experiments. However, except for this particular year in the dataset, in general these quantities appear to be uncorrelated. In contrast, Figure 4b shows a significant correlation between JJA temperature and JJA precipitation (correlation −0.63, $p < .01$), so as expected these quantities are closely related. The correlation between DJFMAM and JJA precipitation is low and not significant (Figure 4c, correlation −0.19, $p > .1$).

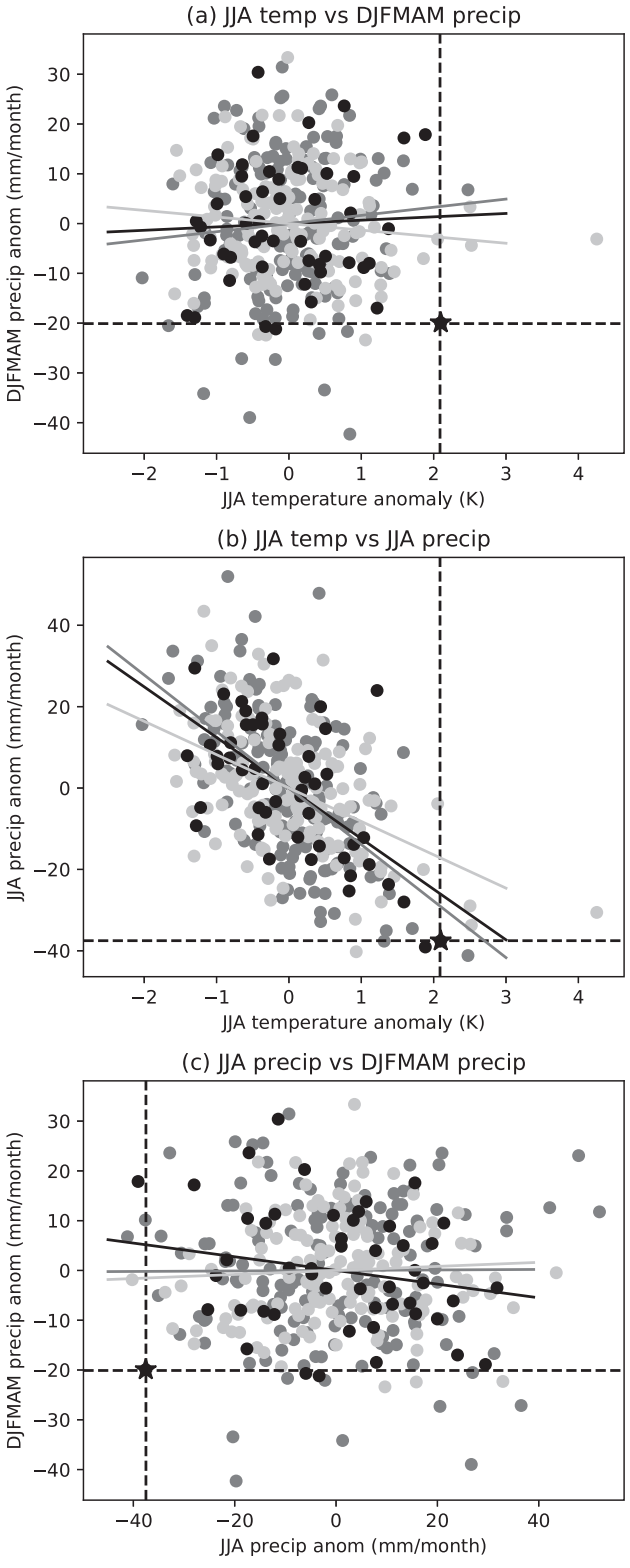

FIGURE 4 Scatter plots of JJA temperature versus (a) preceding DJFMAM precipitation and (b) JJA precipitation in de-trended observations (1950–2000) and model datasets. Black: linearly de-trended observations; light grey: CMIP5 simulations; dark grey: HadGEM3-A simulations. Corresponding lines show the linear fit between the respective datasets; black stars indicate the observed 1975/1976 event; and dashed lines show the respective thresholds of temperature and precipitation

4 | RESULTS

4.1 | Observation-based estimate of the change in likelihood of a 1975/1976 drought and heatwave event

In this section, we discuss the results from the observation-based estimates of the probability of the 1975/1976 drought event, and the change in probability between the climates of 1976 and 2019, using the methodology described in Section 2.1. Local variations in temperature and precipitation are linearly regressed onto the global temperature change trend to provide a signal and noise component, and this is then used to derive distributions of each quantity for the relevant year.

The probability of the 1976 hot summer is estimated to be 0.0097 (confidence interval (CI) [0.0082, 0.012]) in the climate of 1976 (Table 1), where the CI is based on the 5–95% uncertainty range. In other words, it is estimated to be a one-in-103-year event. The estimated probability of the event in the climate of 2019 has decreased significantly since 1976, by a factor of 11 (CI [7,14]) to 0.1 (CI

TABLE 1 Number of events (out of 150), probability and risk ratio of hot summer, dry winter–spring and dry summer for the England and Wales region based on model simulations and observations

	Hot JJA	Dry DJFMAM	Dry JJA
Observation-based			
1976 probability	0.0097 (0.0082–0.012)	0.033 (0.033–0.037)	0.0091 (0.009–0.010)
2019 probability	0.1 (0.063–0.167)	0.014 (0.006–0.034)	0.01 (0.0043–0.024)
Risk ratio	11 (7–14)	0.4 (0.2–0.9)	1.1 (0.5–2.4)
CMIP5			
1970s no. of events	3	3	1
2010s no. of events	26	2	2
1970s probability	0.02	0.02	0.0067
2010s probability	0.173	0.0133	0.0133
Risk ratio	8.7 (4.0–28.0)	0.67 (0.2–3.0)	2 (0.5–4.0)
HadGEM3-A			
1970s no. of events	1	9	2
2010s no. of events	19	7	3
1970s probability	0.0067	0.06	0.0133
2010s probability	0.127	0.047	0.02
Risk ratio	19 (5.0–25.0)	0.8 (0.3–1.8)	1.5 (0.3–5.0)

Note: Dry/hot events are defined as precipitation anomalies being less than the observed anomalies for 1976 (DJFMAM precipitation anomaly less than −20.1 mm·month^{-1}; JJA precipitation anomaly less than −37.5 mm·month^{-1}; JJA temperature anomaly greater than 2.1 K). For risk ratios, the 5–95% uncertainty range based on 1,000 bootstrap samples is shown in brackets.

[0.063,0.167]). This present-day probability is in line with the results of Kay *et al.* (2020), who estimated that the chance of exceeding the 1976 summer UK mean temperature is 13.8% in the 2018 climate. We note that there is some sensitivity of these results to the choice of the GEV fitted distribution (see Section 2). If a Gaussian is used instead, the estimated event probability in 1976 is lower, at around 0.05, while the present-day event probability is unchanged. The probability of the 1975/1976 extreme dry winter–spring is estimated to be 0.033 (CI [0.033,0.037]) in the 1976 climate, that is, a one-in-30-year event. This probability decreases to 0.014 (CI [0.006,0.034]) in the 2019 climate. The risk ratio between these periods is 0.4 (CI [0.2,0.9]), so the reduction in probability is significant based on these uncertainty estimates. For the extreme dry summer of 1976, there is a marginal increase in probability from 0.0091 (CI [0.009,0.01]) in the 1976 climate to 0.01 (CI [0.0043,0.024]) in the 2019 climate. The risk ratio is 1.1 (CI [0.5,2.4]), so this increase is not significant.

The magnitude of these changes is in line with other attribution studies of similar types of events (see, e.g., Stott *et al.* (2004) or Uhe *et al.* (2016) for studies of European summer heatwaves; Wilcox *et al.* (2018) for European precipitation). The relatively large uncertainty ranges are also expected because of the nature of examining extreme events.

4.2 | Climate model-based estimates of the change in likelihood of a 1975/1976 drought and heatwave event

In this section, the probability of the 1975/1976 drought event occurring in the climates of the 1970s and the present day are assessed, using the two different climate model approaches described in Section 2.2.

4.2.1 | Climate model evaluation

Before using the CMIP5 and HadGEM3-A simulations to assess the change in probability of the 1976 event in the present day compared with the 1970s climate, we first evaluate the models against observations.

Vautard *et al.* (2019) gave a detailed evaluation of the HadGEM3-A model in terms of its use for detection and attribution studies. However, note that the model setup used in the present study uses a lower horizontal resolution than that evaluated by Vautard *et al.* (2019) (N96

instead of N216). Vautard *et al.* (2019) found that, overall, the HadGEM3-A model simulates the mean, variability and extremes in Europe fairly well, and concluded that this implied it could be used for attribution studies. However, they show some differences between the observed and modelled trends in temperature and precipitation over the period 1960–2013. They found that the model overestimates the warming trend in Northern Europe in summer, but underestimates the winter warming trend. The observed precipitation increase in Northern Europe in both summer and winter is underestimated by the model. It is worth noting, however, that the observed trends in temperature and precipitation are not all externally forced, as some of these changes will be due to internal variability. It is also of note that, in the EW region, which is the focus of the present study, the modelled trends in summer temperature and precipitation appear to match the observations well.

We now focus on evaluating the HadGEM3-A and CMIP5 models used in the present study. The climatologies of seasonal (winter, spring and summer) mean sea level pressure (MSLP) and wind are shown in Figure 5 for the observations and model simulations. As a proxy for observations, monthly mean wind data from ERA-40 (Uppala *et al.*, 2005) are used, since this has data available back to the 1960s. In general, both model climatologies match the observed climatologies well. However, there are a few minor differences which we discuss now. In

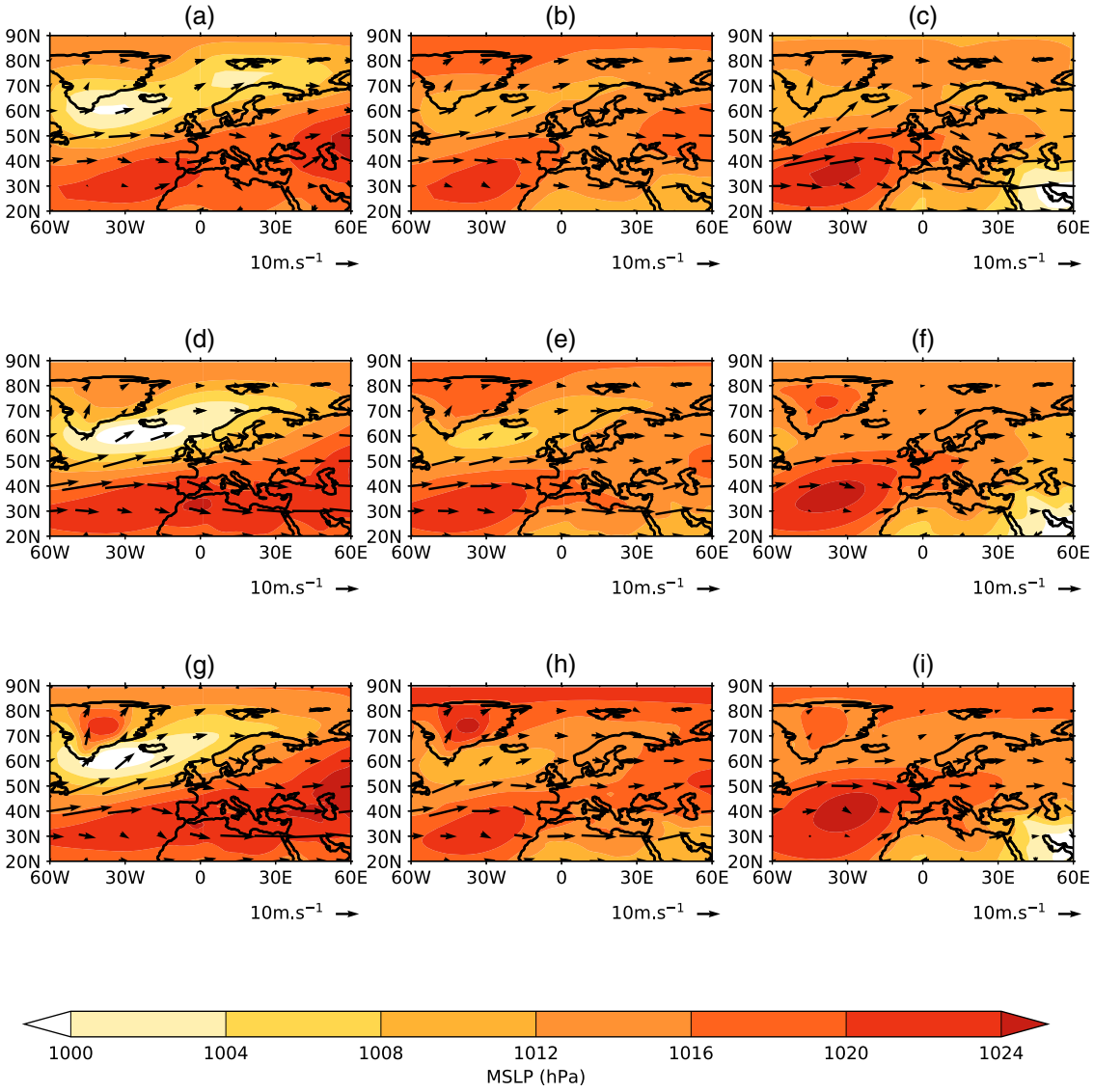

FIGURE 5 Climatology of MSLP and 500 hPa wind for (top) observations for the years 1950/1951 to 1999/2000, (middle) the CMIP5 simulations (mean over 150 simulated years of 1970s) and (bottom) the HadGEM3-A simulations (mean over 150 simulated years of 1976 climate). Left column: DJF, middle column: MAM, right column: JJA. In the top panels, winds are the 1961–1990 mean from ERA-40, re-gridded to the HadGEM3-A grid [Colour figure can be viewed at wileyonlinelibrary.com]

winter, both model climatologies have a slightly stronger north–south pressure gradient than the observations and, correspondingly, a slightly stronger jet. In spring, the model climatologies show slightly stronger winds over the Mediterranean region than in the observed climatology, and weaker winds over Scandinavia, indicating that the jet may be located too far south on average. In summer, the model jet is weaker and more zonal than the observed jet.

Histograms of JJA temperature and DJFMAM and JJA precipitation anomalies in the EW region for the linearly de-trended observations and the model simulations are shown in Figure 6. Observations are de-trended in order to remove the warming trend over the time period of observed data used when calculating the anomalies, so that the distributions can be used as a baseline to compare the model distributions to. The observed and model distributions of JJA temperature are similar and are positively skewed (Figure 6a). A two-sample Kolmogorov–Smirnov test shows that the model JJA temperature distributions are not statistically significantly different from the corresponding observed distribution. The distributions of DJFMAM and JJA precipitation are roughly symmetrical (Figure 6b,c) in both the observations and models. The models both have similar distributions to the observations, but have some more positive and negative extreme years than in the observation set. However, the CMIP5 simulations have a slightly more peaked distribution, with more years with precipitation totals in the central bins than observed (i.e., within 10 mm·month^{-1} of the mean). A two-sample Kolmogorov–Smirnov test shows that the model JJA and DJFMAM precipitation distributions are not statistically significantly different from the corresponding observed distributions.

To assess the independence of the DJFMAM precipitation, JJA precipitation and JJA temperature in the model simulations, Figure 4 shows scatter plots for the model datasets and observations, along with the best-fit lines. As for the observations, the model simulations show no significant correlation between DJFMAM precipitation and either JJA temperature or JJA precipitation (Figure 4a,c; correlations less than 0.1, $p > .1$) and a significant correlation between JJA precipitation and JJA temperature (Figure 4b, correlation −0.48 in the CMIP5 simulations and −0.56 in the HadGEM simulations). From this we can conclude that the climate models show the same temporal independence between JJA temperature, JJA precipitation and DJFMAM precipitation in the EW region as observed.

To check that the modelled extreme precipitation and extreme temperature events we are considering are associated with the same circulation patterns as in observations, Figure 7 shows composites of temperature, precipitation and MSLP anomalies in the extreme model years, along with the 1976 observed anomalies. The numbers

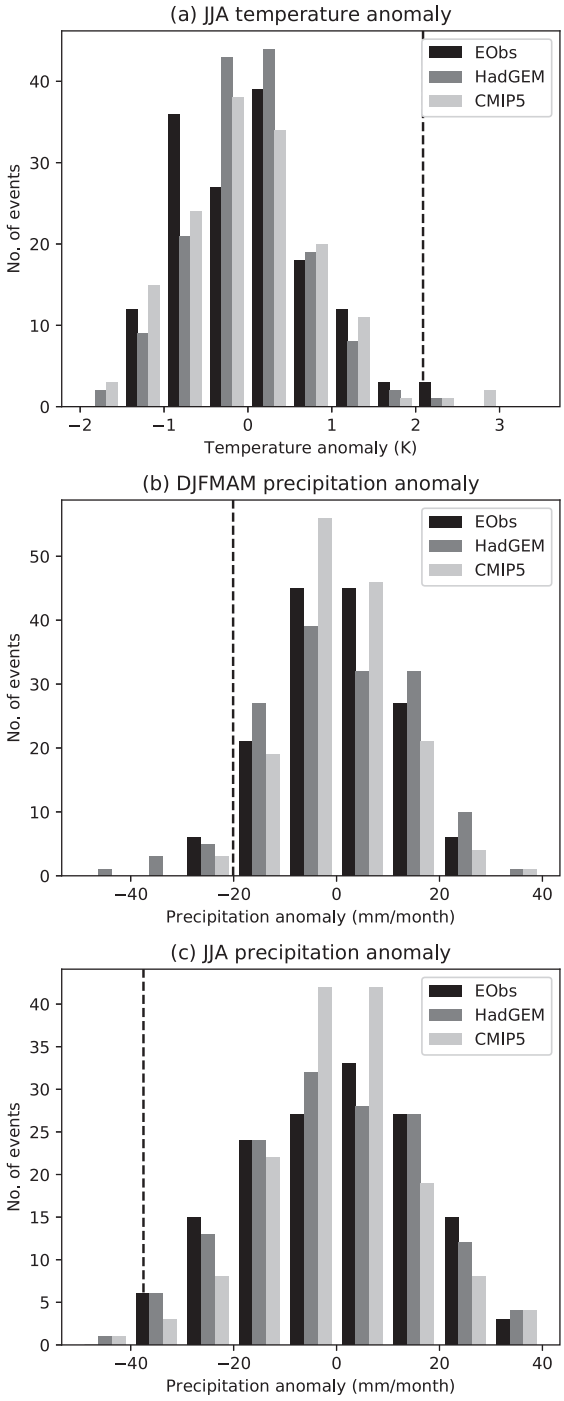

FIGURE 6 Histograms of observed and modelled (a) JJA temperature, (b) DJFMAM precipitation and (c) JJA precipitation anomalies for the England and Wales region, showing the number of events in each bin, out of a total of 150 years for each set (observed values are multiplied by 3 for ease of comparison with model data; there are 50 observed years). Black: E-OBS observations; light grey: CMIP5 simulations of the 1970s; dark grey: HadGEM3-A simulations of the 1970s. Observed anomalies are relative to the mean of the appropriate seasons in 1951–2000 and are de-trended over this period; model anomalies are relative to the model ensemble mean. Black dashed vertical lines show the precipitation and temperature anomaly thresholds. Data are binned every 0.5 K in for temperature, and every 10 mm·month^{-1} for precipitation

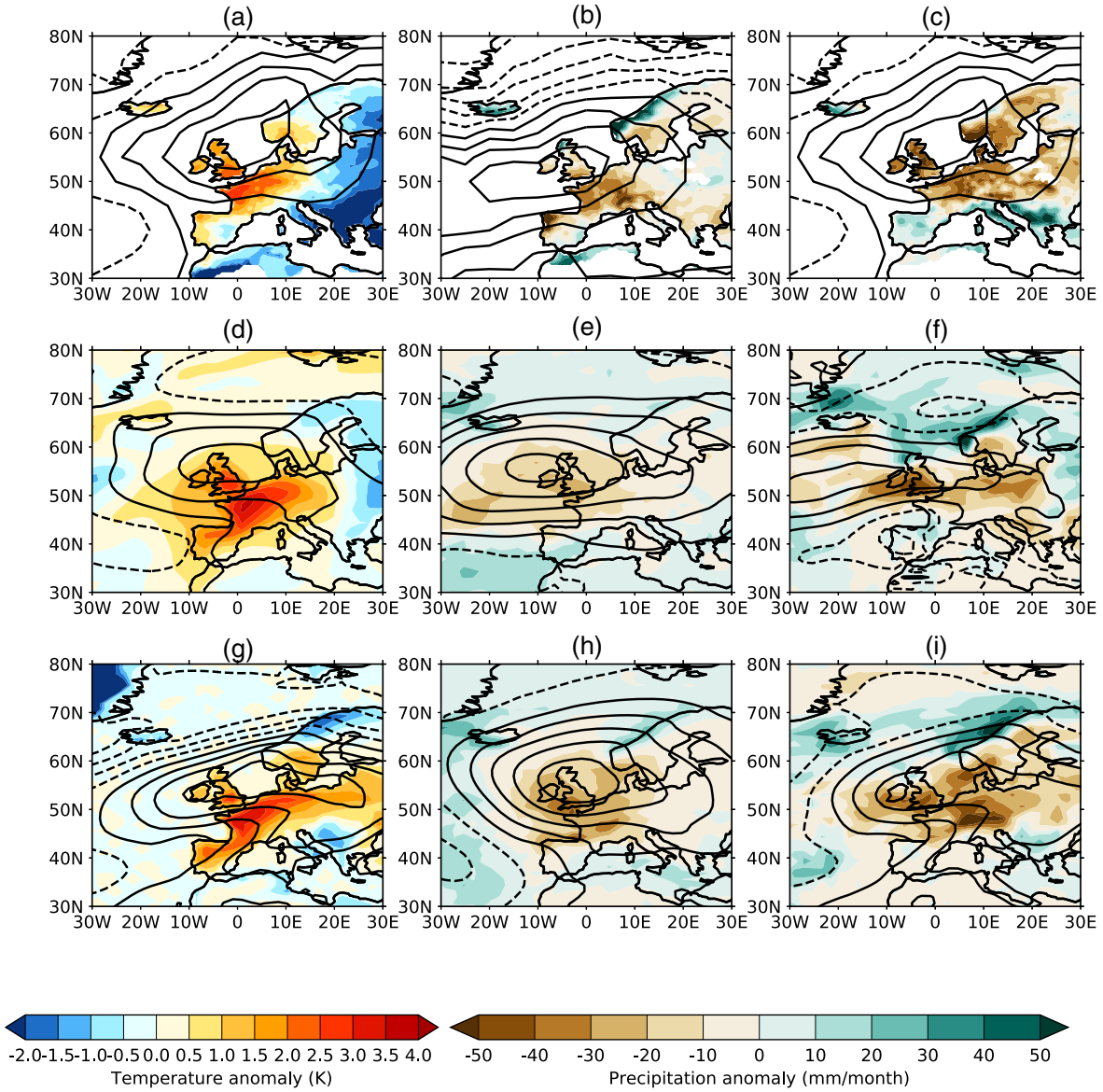

FIGURE 7 Top row: observed anomalies of (a) JJA temperature, (b) DJFMAM precipitation and (c) JJA precipitation in 1975/1976, with contours of MSLP anomalies for the respective periods. Anomalies are relative to the period 1950/1951 to 1999/2000. Middle row: composites of CMIP5 model anomalies, for the years in which the EW box average exceeds the observed thresholds, of (d) JJA temperature, (e) DJFMAM precipitation and (f) JJA precipitation, with corresponding contours of MSLP anomalies. Bottom row: same as the middle row but for the HadGEM3-A simulations. Model anomalies are with respect to the ensemble mean. MSLP contours are shown every 1 hPa, with negative values dashed [Colour figure can be viewed at wileyonlinelibrary.com]

of years included for each model set are listed in Table 1. Overall, the models broadly capture the correct circulation patterns associated with the extreme precipitation and temperature anomalies. However, there are some differences in the precise locations of the anomalies, which are discussed below. The observations of winter–spring 1975/1976 (Figure 7b) show a high pressure anomaly centred just to the west of the UK, with dry anomalies in England and covering most of western Europe, but wet anomalies in northern Scotland and the Norwegian coast. Both model composites show a high pressure anomaly of similar intensity to the observed, but located slightly further north, resulting in the dry anomalies extending to cover the whole of the UK (Figure 7e,h). The strongest precipitation anomalies are, however, still in the southern part of the UK and western Europe, associated with easterly flow from the continent. The observations of summer 1976 (Figure 7a,c) show a high pressure anomaly centred in the North Sea, with positive temperature anomalies covering the whole of the UK and north-west Europe, and dry anomalies covering the whole of northern Europe. The CMIP5 composite of extreme hot JJA

temperatures (Figure 7d) shows a slightly stronger high pressure anomaly centred over Scotland, and a similar pattern of temperature anomalies to the observations. The HadGEM3-A composite of extreme hot JJA temperatures (Figure 7g) shows a high pressure anomaly that extends further to the east than the observed anomaly and, correspondingly, positive temperature anomalies that extend further east over northern Europe. For dry summers, the CMIP5 composite shows a more zonally elongated high pressure anomaly than the observations (Figure 7f), and the precipitation anomalies in eastern Europe are shifted too far south. However, the dry anomaly over much of the UK is well captured, along with a wet anomaly over Spain and Portugal, although there are wet anomalies instead of dry in the north of Scotland. The HadGEM3-A composite (Figure 7i) has the high pressure anomaly in roughly the same position as that observed, and the precipitation anomaly pattern matches the observations well, although the north of Scotland has wet instead of dry anomalies.

4.2.2 | Event probability in 1970s and present-day climates based on CMIP5 and HadGEM3-A simulations

In this section, we use data from the CMIP5 and HadGEM3-A simulations to evaluate the probabilities of the individual components of the 1976 drought and heat event (i.e., extreme high JJA temperature, and extreme low DJFMAM and JJA precipitation) in both the 1970s climate and in the 2010s climate.

Histograms of anomalies of JJA temperature, DJFMAM precipitation and JJA precipitation in the EW region are shown in Figure 8 for both the 1970s and 2010s climates. Both model datasets show a positive shift in the JJA temperature distribution for the EW region (Figure 8a,b). The mean JJA temperature is 1.1 K higher in the 2010s climate than the 1970s climate based on the CMIP5 simulations, and 1.3 K higher based on the HadGEM3 simulations (Figure 9a,b). A two-sample Kolmogorov–Smirnov test shows that the JJA temperature distributions for the two periods are significantly different. In the CMIP5 simulations, the number of events with JJA temperature anomalies exceeding the 1976 observed value increases from 3 in the 1970s climate to 26 in the 2010s climate (Table 1). In the HadGEM3-A simulations, the number of events increases from 1 to 19. This corresponds to a significant increase in probability by a factor of 8.7 (CI [4.0,28.0]) for the CMIP5 simulations and 19 (CI [5.0,25.0]) for the HadGEM3-A simulations (the uncertainties are the 5th to 95th percentile estimates based on 1,000 bootstrap samples). The probability of the 1976 event in terms of JJA temperature has therefore increased from 0.02 to 0.173 based on the CMIP5 results, and from 0.0067 to 0.127 based on the HadGEM3-A results.

Both model datasets show small increases in the mean DJFMAM precipitation of 3.8 mm·month^{-1} in the CMIP5 data and 1.3 mm·month^{-1} in the HadGEM3-A data (Figures 9a and b). The magnitude of these changes is consistent with other studies, for example Vautard *et al.* (2019). A two-sample Kolmogorov–Smirnov test shows that the DJFMAM precipitation distributions in the two periods are not significantly different. For dry winter–spring years with precipitation anomaly less than the 1975/1976 observed anomaly, the CMIP5 simulations show three extreme dry winter–spring periods (with DJFMAM precipitation anomaly less than the 1975/1976 observed anomaly) in the 1970s climate, decreasing to 2 years the 2010s climate (Table 1). The HadGEM3-A simulations show a decrease from 9 to 7 years. The estimated risk ratio for an extreme dry winter–spring period is 0.7 (CI [0.2,3.0]) based on the CMIP5 data and 0.8 (CI [0.3,1.8]) based on the HadGEM3-A data. Both model experiments therefore show a small, but insignificant, decrease in the probability of an extreme dry winter–spring period between the 1970s and 2010s climates.

Both climate model experiments show almost no change in the mean JJA precipitation between the 1970s and 2010s (Figure 9c,d). This is expected from previous studies, for example Wilcox *et al.* (2018). A two-sample Kolmogorov–Smirnov test shows that the JJA precipitation distributions in the two periods are not significantly different. The number of years in the CMIP5 simulations with extreme dry summers (JJA precipitation anomaly less than the 1975/1976 observed anomaly) increases from 1 year in the 1970s climate to 2 years in the 2010s climate (Table 1). In the HadGEM3-A simulations, the number of years increases from 2 to 3 years. The estimated risk ratio for an extreme dry winter–spring period is 2 (CI 0.5,4.0) based on the CMIP5 data and 1.5 (CI 0.3,5.0) based on the HadGEM3-A data. These results indicate that the chance of an extreme dry summer has increased, but this increase is not significant.

In summary, the results from the two climate model-based approaches discussed in this section agree qualitatively with the results from the observation-based estimates shown in Section 4.1. In the EW region, all three methods show that the risk of a winter–spring period drier than that observed in 1975/1976 has decreased. The observations show a slightly larger, and significant, decrease than the climate models, but still within the uncertainty ranges of the model estimates. For the summer season, both model and observation-based estimates show that the risk of a summer drier than that observed in 1976 has increased but not significantly. Finally, all three methods

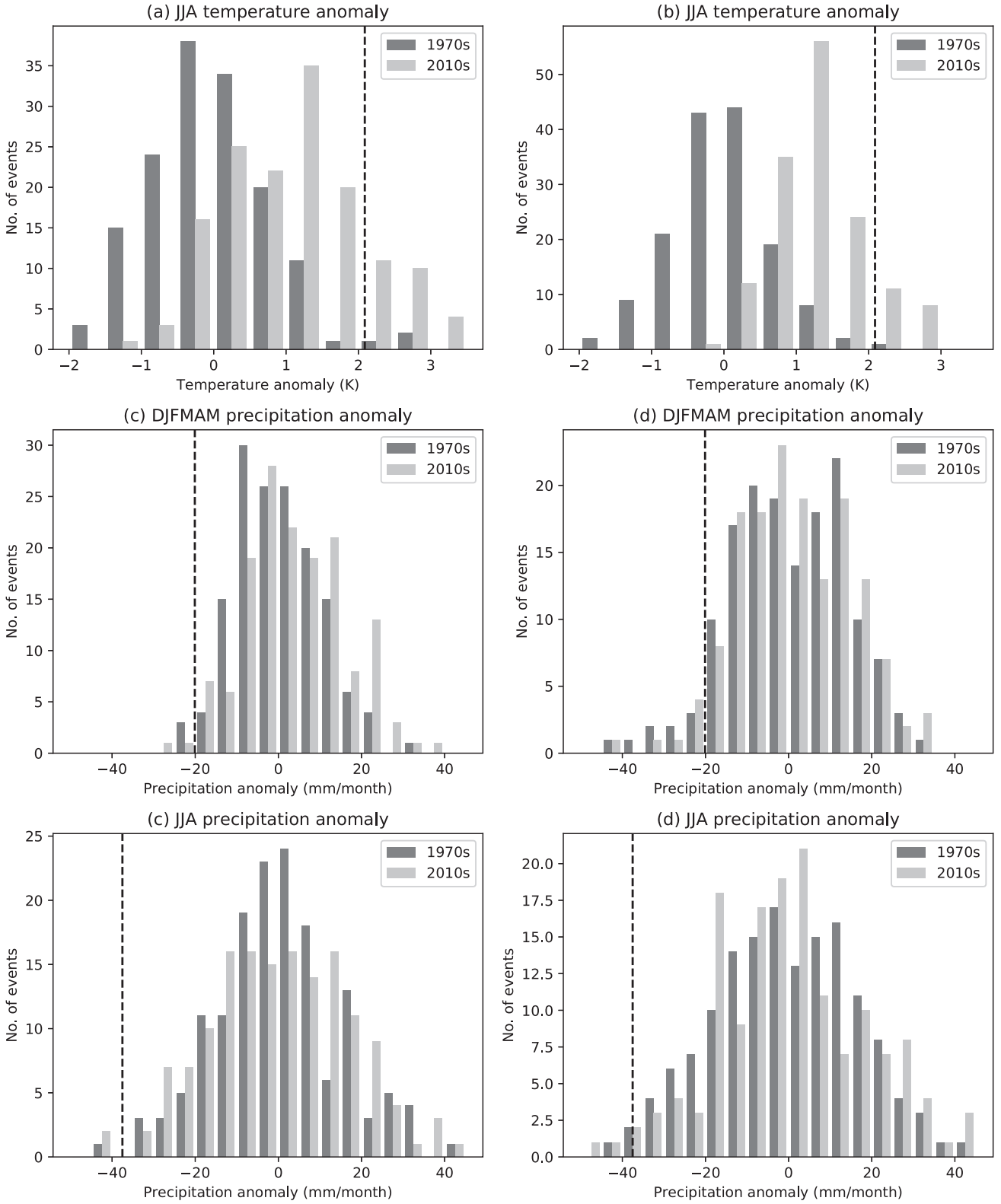

FIGURE 8 Histograms of modelled JJA temperature anomaly (top row), DJFMAM precipitation anomaly (middle row) and JJA precipitation anomaly (bottom row) for the 1970s (dark grey) and 2010s (light grey) climates in the CMIP5 simulations (left column) and the HadGEM3-A simulations (right column). Model anomalies are relative to the model 1970s ensemble mean. Dashed black lines show the corresponding observed anomaly thresholds. Data are binned every 0.5 K in for temperature and every 5 mm·month^{-1} for precipitation

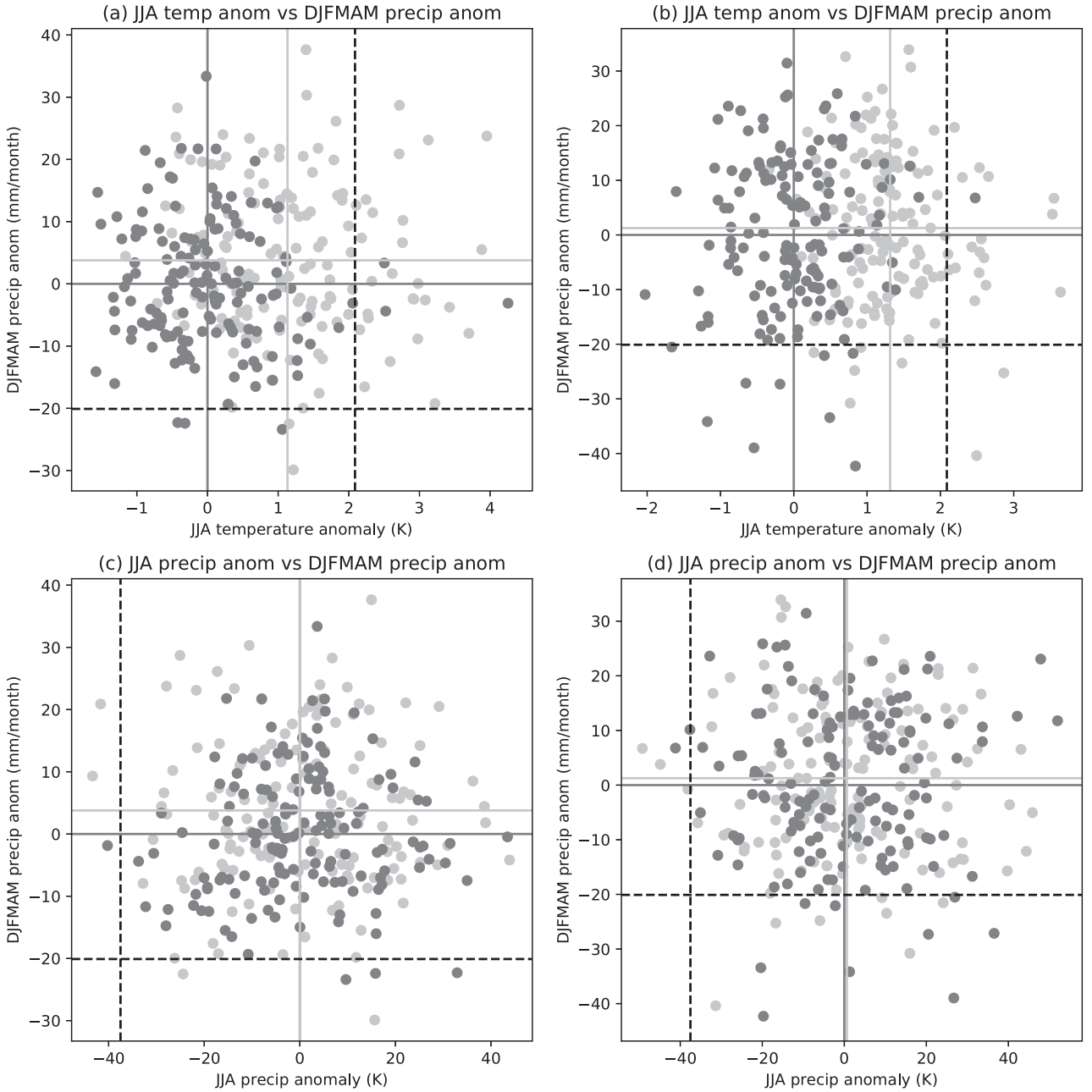

FIGURE 9 Scatter plots of JJA temperature versus preceding DJFMAM precipitation (top row) and versus JJA precipitation (bottom row), for (a,c) the CMIP5 simulations and (b,d) the HadGEM3-A simulations. Dark grey shows 1970s climate and light grey shows 2010s climate. Corresponding horizontal and vertical lines show the means for each quantity. Dashed black lines show the observed thresholds

agree that the risk of JJA temperatures exceeding those observed in summer 1976 has increased significantly. In particular, the hot summer of 1976 would no longer be considered extreme in the recent decade, as it is estimated to be a one-in-6 to one-in-10-year event. This significant increase in heatwave likelihood is consistent with the results of Kay *et al.*, (2020). In Section 5, we discuss the probabilities of the combined occurrence of these aspects, and the implications of these results.

4.3 | Sensitivity to precipitation and temperature thresholds

The results presented so far have been based on using the 1975/1976 observed temperature and precipitation anomalies as the thresholds for defining the event. Given that we are examining what is considered to be one of the most extreme drought and heatwave events in north-western Europe in historical record, the number of occurrences

TABLE 2 Combined event probabilities for the England and Wales region calculated using bivariate copulas

	Dry DJFMAM, hot JJA	dry DJFMAM, dry JJA	dDry JJA, hot JJA
CMIP5			
1970s probability	0.0005 (0.0002–0.0009)	0.00023 (0–0.0005)	0.0002 (0–0.0004)
2010s probability	0.0051 (0.0038–0.0061)	0.00030 (0–0.0005)	0.0016 (0.0009–0.0024)
Risk ratio	13.3 (5.3–27.2)	1.8 (0.33–5.0)	10.2 (3.0–20.0)
HadGEM3-A			
1970s probability	0.00031 (0–0.0006)	0.000777 (0.000295–0.0014)	0.000036 (0–0.0001)
2010s probability	0.0069 (0.0055–0.0085)	0.0015 (0.0009–0.0023)	0.0028 (0.0017–0.0039)
Risk ratio	33.1 (10.9–79.1)	2.6 (0.9–6.3)	28.1 (16.0–39.0)

Note: Probability and risk ratio of the combined occurrence of extreme dry winter–spring followed by an extreme hot summer; extreme dry winter–spring followed by an extreme dry summer and of an extreme hot and dry summer. The results are based on the Archimedean Frank bivariate copula fitted to the data from the climate model simulations. Dry/hot events are defined as precipitation anomalies being less than/greater than the observed anomalies for 1976 (DJFMAM precipitation anomaly less than $-20.1\ \text{mm}\cdot\text{month}^{-1}$; JJA precipitation anomaly less than $-37.5\ \text{mm}\cdot\text{month}^{-1}$ and JJA temperature anomaly greater than 2.1 K).

will by definition be very small. The return period curves in Figure S1 in the supplementary information show the return periods for exceeding each temperature value (top row), and precipitation being less than each precipitation value (middle and bottom rows), for the two model datasets. Black dashed lines show the observed 1975/1976 values, which were used as the event thresholds in the previous sections. The grey dashed lines indicate the *n*th most extreme years in the 50-year de-trended observed series, where *n* ranges from 1 to 10. By definition, the return period of an event reduces as the magnitude of the threshold is reduced (i.e., as the event becomes less extreme). However, it is of interest to see how sensitive the risk ratios are to these changes in thresholds. These results are shown in Figure S2 in the supplementary information. The thresholds used are the *n*th most extreme years in the 50-year de-trended observed series, where *n* ranges from 1 to 10. The 10th most extreme values therefore define the upper (lower) quintile for the temperature (precipitation) series. For hot JJA, the risk ratios and 5–95% confidence ranges are above 1 for both model datasets and for all thresholds shown, so the fact that there is a significant increase in probability is not sensitive to the choice of threshold. There is a general decrease in risk ratio as the temperature threshold decreases, but the results are generally within the uncertainty range of the estimated risk ratios obtained in Section 4. For dry DJFMAM, the risk ratios are relatively similar for all thresholds, and the uncertainty ranges decrease for the least extreme thresholds. The choice of threshold does not change the overall results that the likelihood of the event has decreased, but not significantly (with the exception of the second to fourth most extreme thresholds which show an insignificant increase in probability based on the CMIP5 simulations). For dry JJA, the risk ratios show an overall slight decrease as the threshold is weakened, and a reduction in the uncertainty range. The HadGEM3-A results show a change in the estimated risk ratio from above 1 to below 1 for the weaker precipitation thresholds, but the uncertainty ranges show that these changes are again not significant.

5 | ASSESSING THE CHANGE IN PROBABILITY OF JOINT OCCURRENCE OF DIFFERENT ASPECTS OF THE 1975/1976 DROUGHT EVENT

In Section 4, we considered the three key components of the 1975/1976 drought event separately, namely the winter–spring precipitation, which is important for water supply, and the summer temperature and precipitation, which mainly affect water demand (although in years of high summer precipitation such as summer 2012 this can also contribute to groundwater recharge in the UK). The most severe impacts are often a result of a combination of two or more factors occurring in the same year, and it was the combination of these three factors that made the 1976 event so exceptional. It is therefore of interest to consider the probability of two or more of these components occurring in the same year. Due to the extreme nature of the 1975/1976 event, in our model simulations we find only one event where both the JJA temperature and JJA precipitation thresholds were exceeded (Figure 4b), and no events where both the DJFMAM precipitation and either JJA thresholds were exceeded (Figure 4a,c). This is not surprising given the limited sample size and the fact that these

are extreme events and, therefore, by definition occur infrequently. However, it means that we cannot estimate the change in combined probabilities simply by finding years in the model output in which two or three threshold criteria were passed.

Instead, bivariate copulas are used. This is a method of deriving a joint distribution function from two datasets. In this case, the various pairs of data from the climate model estimates of DJFMAM precipitation, JJA precipitation and JJA temperature are used to derive the copulas. Bivariate copulas have been used in other similar studies, for example Zscheischler and Fischer (2020), and their formulation and use is described in detail by Salvadori *et al.* (2016) and references therein. The Archimedean Frank copula (Mai and Scherer, 2013) was found to be appropriate for each pair of variables, and passed a goodness-of-fit test when fitted to the climate model data. The derived bivariate copulas were used to compute the probabilities and risk ratios for exceeding the bivariate thresholds of the respective quantities.

The results obtained using this method are presented in Table 2. The estimated probabilities are generally small, which is expected given that the individual components alone are extreme events, so the combined occurrence will be even more extreme. For a dry winter–spring followed by a hot summer, the probability is estimated to have increased significantly between the 1970s and 2010s by a factor of around 13 (CI [5.3,27.2]) based on the CMIP5 model simulations and 33 (CI [10.9,79.1]) based on the HadGEM3-A simulations. Similarly, for a dry and hot summer, there is also a significant increase in probability between the two periods, by a factor of 10 (CI [3.0,20.0]) based on the CMIP5 model simulations and 28 (CI [16.0,39.0]) based on the HadGEM3-A simulations. The probability of a dry winter–spring and dry summer has increased but not significantly: the CMIP5 simulations show a risk ratio of 1.8 (CI [0.33,5]), and the HadGEM3-A simulations show a risk ratio of 2.6 (CI [0.9,6.3]).

6 | CONCLUSIONS

6.1 | Summary of results

The summer of 1976 was exceptionally hot and dry in north-west Europe, and was also preceded by a prolonged dry period. The England and Wales region of the UK experienced a severe drought, which is considered to be a benchmark drought event. The aim of this study was to assess the change in likelihood of a 1975/1976 drought and heatwave event in the present-day climate compared with that of 1976. Three different methods were used to achieve this: one based on observations, a second based on coupled climate model simulations (CMIP5) and a third based on atmosphere-only climate model simulations (HadGEM3-A). The methodologies followed the principles of event attribution to assess the probability of the extreme events occurring in the different climates. To the authors' knowledge, this is the first time that the attribution methodology used in this study has been used to assess whether the likelihood of a historical extreme benchmark event has changed due to climate change between the period in which it occurred and the present day. This method could also be applied to other events which are used as benchmark events for planning purposes, for example the 2003 European heatwave.

The 1975/1976 drought event was defined based on three key components: the dry winter–spring period, the dry summer and the hot summer. The observed 1975/1976 precipitation and temperature anomalies were used as thresholds, and the event was based on exceeding these thresholds. The results based on the three different approaches agreed well with each other, further adding confidence to the robustness of our results.

The results from this study suggest that the probability of a summer as hot as that of 1976 is now significantly higher than it was in the 1970s climate (combining results from the three methods, the probability has increased by a factor of between 4 and 28). In particular, based on these results, such an extreme hot summer in the current climate is no longer considered to be "extreme". The probability of an extreme dry winter–spring period has decreased, but not significantly, while the probability of an extreme dry summer has increased, but again not significantly. The joint probabilities of combined occurrence of pairs of factors of the extreme event were also considered. The likelihood of an extreme dry winter–spring followed by an extreme hot summer has increased significantly (combined risk ratio estimate between 5 and 79). The likelihood of an extreme hot and dry summer has also increased significantly (combined risk ratio estimate between 3 and 39). No significant change was found in the likelihood of an extreme dry winter–spring followed by an extreme dry summer (combined risk ratio estimate between 0.3 and 6.3).

6.2 | Implications for water management and water supply

The winter–spring precipitation is important for recharging groundwater and surface water stores which are key for the UK's water supply system. This means that, at the end of an extreme dry winter–spring period (such as that of 1975/1976), the groundwater and surface water

reserves will be low. An extreme hot summer will create an increased water demand, and further loss of water resource through increased evaporation. Therefore, an extreme hot summer following a dry winter–spring period will put increased demand on the already depleted groundwater and surface water reserves.

The 1975/1976 drought is considered in the UK as a benchmark extreme drought event, and there is an implicit assumption that the probability of such an event has not changed since the 1970s. The results of this study show that the probability of a summer as hot as 1976 has increased significantly, as have the joint probability of an extreme dry winter–spring period followed by an extreme hot summer and the probability of an extreme hot and dry summer. Water resource systems should therefore be resilient enough to cope with an increased incidence of extreme dry winter–spring periods followed by extreme hot summers comparable to that of 1975/1976. For the agricultural sector, the significant increase in the chance of extreme hot, dry summers means that the demand for water for irrigation will be higher, and there is a potential negative impact on rain-fed crops. However, severe restrictions on water use are likely to be more common, which may mean that water for additional irrigation is more limited. In terms of the public water supply, the increased likelihood of an event as severe as 1976 means that it is increasingly important that the water supply systems be resilient enough to be able to cope with an extreme dry winter–spring period followed by an extreme hot summer, without needing to apply restrictions to public water supply, as was necessary in 1976.

AUTHOR CONTRIBUTIONS

Laura Baker: data curation; formal analysis; investigation; methodology; visualization; writing – original draft; writing – review and editing. **Len Shaffrey:** conceptualization; funding acquisition; supervision; writing – review and editing. **Ed Hawkins:** formal analysis; investigation; writing – review and editing.

ACKNOWLEDGEMENTS

L. Baker was funded by NERC grant number NE/L010488/1 (IMPETUS project) and EUPHEME Project (Grant Number: Grant 690462). This work was supported by the National Centre for Atmospheric Science.

DATA ACCESS STATEMENT

The data from the HadGEM3-A simulations can be accessed on JASMIN. Please see the supporting information for further details.

ORCID

Laura Baker https://orcid.org/0000-0003-0738-9488

REFERENCES

Alexander, L. (2011) Extreme heat rooted in dry soils. *Nature Geoscience*, 4, 12–13.

Allan, R. and Ansell, T. (2006) A new globally complete monthly historical gridded mean sea level pressure dataset (HadSLP2): 1850-2004. *Journal of Climate*, 19, 5816–5842.

Dunstone, N., Smith, D., Hardiman, S., Eade, R., Gordon, M., Hermanson, L., Kay, G. and Scaife, A. (2019) Skilful real-time seasonal forecasts of the dry northern European summer 2018. *Geophysical Research Letters*, 46, 12368–12376.

Fischer, E.M., Seneviratne, S.I., Lüthi, D. and Schär, C. (2007) Contribution of land-atmosphere coupling to recent European summer heat waves. *Geophysical Research Letters*, 34

Folland, C.K., Knight, J., Linderholm, H.W., Fereday, D., Ineson, S. and Hurrell, J.W. (2009) The summer North Atlantic Oscillation: past, present, and future. *Journal of Climate*, 22, 1082–1103.

Hauser, M., Gudmundsson, L., Orth, R., Jézéquel, A., Haustein, K., Vautard, R., Van Oldenborgh, G.J., Wilcox, L. and Seneviratne, S.I. (2017) Methods and model dependency of extreme event attribution: the 2015 European drought. *Earth's Future*, 5, 1034–1043.

Hawkins, E., Frame, D., Harrington, L., Joshi, M., King, A., Rojas, M. and Sutton, R. (2020) Observed emergence of the climate change signal: from the familiar to the unknown. *Geophysical Research Letters*, 47, e2019GL086259

Haylock, M., Hofstra, N., Klein Tank, A., Klok, E., Jones, P. and New, M. (2008) A European daily high-resolution gridded data set of surface temperature and precipitation for 1950–2006. *Journal of Geophysical Research: Atmospheres*, 113

Kay, G., Dunstone, N., Smith, D., Dunbar, T., Eade, R. and Scaife, A. (2020) Current likelihood and dynamics of hot summers in the UK. *Environmental Research Letters*, 15, 094099.

Kendon, M., McCarthy, M., Jevrejeva, S., Matthews, A. and Legg, T. (2019) State of the UK climate 2018. *International Journal of Climatology*, 39, 1–55.

Kendon, M., McCarthy, M., Jevrejeva, S., Matthews, A., Sparks, T. and Garforth, J. (2020) State of the UK climate 2019. *International Journal of Climatology*, 40, 1–69. https://doi.org/10.1002/joc.6726.

Kennedy, J.J., Rayner, N.A., Smith, R.O., Parker, D.E. and Saunby, M. (2011) Reassessing biases and other uncertainties in sea surface temperature observations measured in situ since 1850: 1. measurement and sampling uncertainties. *Journal of Geophysical Research*, 116. https://doi.org/10.1029/2010JD015218.

Lewis, S.C. and Karoly, D.J. (2013) Anthropogenic contributions to Australia's record summer temperatures of 2013. *Geophysical Research Letters*, 40, 3705–3709.

Mai, J.-F. and Scherer, M. (2013) *Simulating Copulas: Stochastic Models, Sampling Algorithms, and Applications*. London: Imperial College Press.

Marsh, T., Cole, G. and Wilby, R. (2007) Major droughts in England and Wales, 1800–2006. *Weather*, 62, 87–93.

Murray, R. (1977) The 1975/76 drought over the United Kingdom - hydrometeorological aspects. *Meteorological Magazine*, 106, 129–145.

van Oldenborgh, G.J., Mitchell-Larson, E., Vecchi, G.A., de Vries, H., Vautard, R. and Otto, F. (2019) Cold waves are getting milder in the northern midlatitudes. *Environmental Research Letters*, 14, 114004. https://doi.org/10.1088/1748-9326/ab4867.

van Oldenborgh, G.J., van der Wiel, K., Kew, S., Philip, S., Otto, F., Vautard, R., King, A., Lott, F., Arrighi, J., Singh, R. and van Aalst, M. (2021) Pathways and pitfalls in extreme event attribution. *Climatic Change*, 166, 1–27. https://doi.org/10.1007/s10584-021-03071-7.

Otto, F.E., van der Wiel, K., van Oldenborgh, G.J., Philip, S., Kew, S.F., Uhe, P. and Cullen, H. (2018) Climate change increases the probability of heavy rains in northern England/southern Scotland like those of storm Desmond—a real-time event attribution revisited. *Environmental Research Letters*, 13, 024006

Pall, P., Aina, T., Stone, D.A., Stott, P.A., Nozawa, T., Hilberts, A.G., Lohmann, D. and Allen, M.R. (2011) Anthropogenic greenhouse gas contribution to flood risk in England and Wales in autumn 2000. *Nature*, 470, 382

Perry, A.H. (1976) The long drought of 1975–76. *Weather*, 31, 328–336.

Ratcliffe, R.A.S. (1977) A synoptic climatologist's viewpoint of the 1975/76 drought. *Meteorological Magazine*, 106, 145–154.

Rayner, N.A., Parker, D.E., Horton, E.B., Folland, C.K., Alexander, L.V., Rowell, D.P., Kent, E.C. and Kaplan, A. (2003) Global analyses of sea surface temperature, sea ice, and night marine air temperature since the late nineteenth century. *Journal of Geophysical Research*, 108

Rodda, J. and Marsh, T. (2011) *The 1975-76 Drought–A Contemporary and Retrospective Review*. Wallingford, UK: Centre for Ecology and Hydrology. Technical Report 58.

Rohde, R., Muller, R.A., Jacobsen, R., Muller, E., Perlmutter, S., Rosenfeld, A., Wurtele, J., Groom, D. and Wickham, C. (2013) A new estimate of the average earth surface land temperature spanning 1753 to 2011. *Geoinformatics and Geostatistics*, 1.

Salvadori, G., Durante, F., De Michele, C., Bernardi, M. and Petrella, L. (2016) A multivariate copula-based framework for dealing with hazard scenarios and failure probabilities. *Water Resources Research*, 52, 3701–3721.

Schaller, N., Kay, A.L., Lamb, R., Massey, N.R., Van Oldenborgh, G.J., Otto, F.E., Sparrow, S.N., Vautard, R., Yiou, P., Ashpole, I., Bowery, A., Crooks, S.M., Haustein, K., Huntingford, C., Ingram, W.J., Jones, R.G., Legg, T., Miller, J., Skeggs, J., Wallom, D., Weisheimer, A., Wilson, S., Stott, P.A. and Allen, M.R. (2016) Human influence on climate in the 2014 southern England winter floods and their impacts. *Nature Climate Change*, 6, 627.

Sippel, S., Otto, F.E., Flach, M. and van Oldenborgh, G.J. (2016) The role of anthropogenic warming in 2015 central European heat waves. *Bulletin of the American Meteorological Society*, 97, S51–S56.

Stefanon, M., D'Andrea, F. and Drobinski, P. (2012) Heatwave classification over Europe and the Mediterranean region. *Environmental Research Letters*, 7, 014023

Stocker, T., Qin, D., Plattner, G.-K., Tignor, M., Allen, S., Boschung, J., Nauels, A., Xia, Y., Bex, V. and Midgley, P. (Eds.) (2014) *Climate Change 2013: The Physical Science Basis: Working Group I Contribution to the Fifth Assessment Report of the Intergovernmental Panel on Climate Change*. Cambridge: Cambridge University Press.

Stott, P.A., Christidis, N., Otto, F.E., Sun, Y., Vanderlinden, J.-P., Van Oldenborgh, G.J., Vautard, R., Von Storch, H., Walton, P., Yiou, P. and Zwiers, F.W. (2016) Attribution of extreme weather and climate-related events. *Wiley Interdisciplinary Reviews: Climate Change*, 7, 23–41.

Stott, P.A., Stone, D.A. and Allen, M.R. (2004) Human contribution to the European heatwave of 2003. *Nature*, 432, 610–614.

Stubbs, M.W. (1977) Exceptional European weather in 1976. *Weather*, 32, 457–463. https://doi.org/10.1002/j.1477-8696.1977.tb04504.x.

Taylor, K.E., Stouffer, R.J. and Meehl, G.A. (2012) An overview of CMIP5 and the experiment design. *Bulletin of the American Meteorological Society*, 93, 485–498.

Taylor, V., Chappells, H., Medd, W. and Trentmann, F. (2009) Drought is normal: the socio-technical evolution of drought and water demand in England and Wales, 1893–2006. *Journal of Historical Geography*, 35, 568–591.

Uhe, P., Otto, F.E.L., Haustein, K., van Oldenborgh, G.J., King, A.D., Wallom, D.C.H., Allen, M.R. and Cullen, H. (2016) Comparison of methods: attributing the 2014 record European temperatures to human influences. *Geophysical Research Letters*, 43, 8685–8693.

Uppala, S.M., Kållberg, P., Simmons, A., Andrae, U., Bechtold, V.D.C., Fiorino, M., Gibson, J., Haseler, J., Hernandez, A., Kelly, G. and et al. (2005) The ERA-40 re-analysis. *Quarterly Journal of the Royal Meteorological Society*, 131, 2961–3012.

Vautard, R., van Aalst, M., Boucher, O., Drouin, A., Haustein, K., Kreienkamp, F., van Oldenborgh, G.J., Otto, F.E.L., Ribes, A., Robin, Y., Schneider, M., Soubeyroux, J.-M., Stott, P., Seneviratne, S.I., Vogel, M.M. and Wehner, M. (2020) Human contribution to the record-breaking June and July 2019 heatwaves in Western Europe. *Environmental Research Letters*, 15, 094077. https://doi.org/10.1088/1748-9326/aba3d4.

Vautard, R., Christidis, N., Ciavarella, A., Alvarez-Castro, C., Bellprat, O., Christiansen, B., Colfescu, I., Cowan, T., Doblas-Reyes, F., Eden, J., Hauser, M., Hegerl, G., Hempelmann, N., Klehmet, K., Lott, F., Nangini, C., Orth, R., Radanovics, S., Seneviratne, S.I., van Oldenborgh, G.J., Stott, P., Tett, S., Wilcox, L. and Yiou, P. (2019) Evaluation of the HadGEM3-A simulations in view of detection and attribution of human influence on extreme events in Europe. *Climate Dynamics*, 52, 1187–1210.

Vautard, R., Yiou, P., D'Andrea, F., de Noblet, N., Viovy, N., Cassou, C., Polcher, J., Ciais, P., Kageyama, M. and Fan, Y. (2007) Summertime European heat and drought waves induced by wintertime Mediterranean rainfall deficit. *Geophysical Research Letters*, 34.

Walters, D., Baran, A.J., Boutle, I., Brooks, M., Earnshaw, P., Edwards, J., Furtado, K., Hill, P., Lock, A., Manners, J., Morcrette, C., Mulcahy, J., Sanchez, C., Smith, C., Stratton, R., Tennant, W., Tomassini, L., Van Weverberg, K., Vosper, S., Willett, M., Browse, J., Bushell, A., Carslaw, K., Dalvi, M., Essery, R., Gedney, N., Hardiman, S., Johnson, B., Johnson, C., Jones, A., Jones, C., Mann, G., Milton, S., Rumbold, H., Sellar, A., Ujiie, M., Whitall, M., Williams, K. and Zerroukat, M. (2019) The Met Office Unified Model Global Atmosphere 7.0/7.1 and JULES Global Land 7.0 configurations. *Geoscientific Model Development*, 12, 1909–1963.

Walters, D., Best, M., Bushell, A., Copsey, D., Edwards, J., Falloon, P., Harris, C., Lock, A., Manners, J., Morcrette, C., Roberts, M., Stratton, R., Webster, S., Wilkinson, J., Willett, M., Boutle, I., Earnshaw, P., Hill, P., MacLachlan, C., Martin, G., Moufouma-Okia, W., Palmer, M., Petch, J., Rooney, G., Scaife, A. and Williams, K. (2011) The Met Office Unified Model global atmosphere 3.0/3.1 and JULES global land 3.0/3.1 configurations. *Geoscientific Model Development*, 4, 919–941.

Whan, K., Zscheischler, J., Orth, R., Shongwe, M., Rahimi, M., Asare, E.O. and Seneviratne, S.I. (2015) Impact of soil moisture on extreme maximum temperatures in Europe. *Weather and Climate Extremes*, 9, 57–67.

Wilcox, L.J., Yiou, P., Hauser, M., Lott, F.C., van Oldenborgh, G.J., Colfescu, I., Dong, B., Hegerl, G., Shaffrey, L. and Sutton, R. (2018) Multiple perspectives on the attribution of the extreme European summer of 2012 to climate change. *Climate Dynamics*, 50, 3537–3555.

Williams, A.P., Seager, R., Abatzoglou, J.T., Cook, B.I., Smerdon, J.E. and Cook, E.R. (2015) Contribution of anthropogenic warming to California drought during 2012–2014. *Geophysical Research Letters*, 42, 6819–6828.

Zscheischler, J. and Fischer, E.M. (2020) The record-breaking compound hot and dry 2018 growing season in Germany. *Weather and Climate Extremes*, 29, 100270

SUPPORTING INFORMATION

Additional supporting information may be found online in the Supporting Information section at the end of this article.

How to cite this article: Baker, L., Shaffrey, L. & Hawkins, E. (2021) Has the risk of a 1976 north-west European summer drought and heatwave event increased since the 1970s because of climate change?. *Quarterly Journal of the Royal Meteorological Society*, 1–20. Available from: https://doi.org/10.1002/qj.4172